Redox-initiated radical decomposition of triazenes and their platinum complexes studied by cyclic voltammetry and EPR spectroscopy

Peter Rapta,[a] Ladislav Omelka,[a] Andrej Staško,*[a] Jochen Dauth,[b] Bernward Deubzer[b] and Johann Weis[b]

[a] Department of Physical Chemistry, Slovak Technical University, SK-812 37 Bratislava, Slovak Republic
[b] Wacker Chemie GmbH, Burghausen, D-84480 Germany

Triazenes p-R^1-C_6H_4-N=N-NR^2R^3 (R^1 = H, butyl, CH_3O, CN and NO_2, R^2 = CH_3, cyclohexyl, butyl or longer chains, R^3 = H, OH) are irreversibly cathodically reduced at -1.5 to -2.7 V ($vs.$ saturated calomel electrode) and oxidised from 0.8 to 1.7 V. The reduction peak potentials became more negative and the first oxidation peak potentials less positive if R^3 was OH. Using spin-trapping, radicals p-R^1-C_6H_4· and ·R^2 were identified as fragmentation products in the electrolytic and peroxy-initiated decomposition of triazenes. Radicals p-$R^1C_6H_4$-NO·-R^2, representing the oxidised cage products after N_2 elimination, were observed in the oxidation of triazenes with peroxy acid. An NO_2-centred radical anion was found in the cathodic reduction of a Pt complex with R^1 = NO_2. The above specified decomposition route of triazenes is modified if these are coordinated in Pt complexes. The formation of radicals is discussed assuming two tautomeric forms of triazenes.

Triazenes increasingly find applications as initiators of radical polymerisation,[1] promoters of polymer ablation by ultraviolet irradiation[2] and also as antitumour drugs (see e.g. ref. 3). Recent interest in these compounds and their platinum complexes is based on the search for highly reactive platinum fragments as catalysts for hydrosilylation reactions.[4] Therefore, the fragmentation pattern of substituted phenylalkyltriazenes and their corresponding tetrakis(phenylalkyltriazenido)-Pt[IV] complexes attracts much attention. The decomposition of symmetrical dialkyltriazenes in acidic aqueous solution proceeds with formation of alkylamines and alkyl alcohols via alkyldiazonium intermediates, whereas asymmetric 1,3-dialkyltriazenes preferably form different alkyldiazonium ions and alkylamines due to two tautomeric forms in the starting triazenes.[5] In electrochemical oxidation of 1,3-diphenyltriazene, intermediate formation of the triazene cation radical was assumed, which after protonation with residual water rearranges to aniline and finally converts to p-aminoazobenzene. In the case of 3,3-dimethyl-1-phenyltriazene a phenyldiazonium ion and dimethylamine are formed.[6a] Recently,[6b] one electron anodic oxidation of variously phenyl-substituted 3,3-dimethyl-1-phenyltriazenes and 3-methyl-1,3-phenyltriazenes was described. In our study the redox properties of asymmetric 1-phenyl-3-alkyltriazenes and their corresponding triazenido-platinum complexes are characterised by cyclic voltammetry. The structure of radical intermediates formed in electrolytic reactions and in oxidation with peroxy compounds is investigated using EPR spectroscopy. The mechanism for the formation of radicals is discussed.

Experimental

The investigated triazenes 1, 2 and their Pt complexes 3, 4 (Table 1) were prepared as described in ref. 7. The solvents acetonitrile (ACN), benzene, dichloromethane and other chemicals were of analytical grade purity from commercial sources. Tetrabutylammonium perchlorate (TBAP), $LiClO_4$, spin traps 2-methyl-2-nitrosopropane (Bu^{t}NO), nitrosodurene (ND) and 5,5-dimethyl-1-pyrroline N-oxide (DMPO) were from Sigma, DMPO was freshly distilled before use and kept at -25 °C.

The cyclovoltammetric investigations were carried out in a 0.001 mol dm^{-3} probe, 0.1 mol dm^{-3} TBAP in acetonitrile or in special cases in dichloromethane solutions (to confirm the observed radicals do not originate from ACN) using a universal electrochemical system: Princeton Applied Research 270 (PAR 270). The in-house constructed electrochemical cell consisted of platinum wire working and auxiliary tin electrodes. A saturated calomel electrode (SCE) placed in a separate compartment with a carbon joint served as a reference.
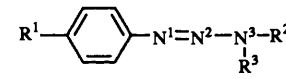
The electrochemically initiated decomposition of triazenes was carried out directly in the cavity of a Bruker 200 E-SRC EPR spectrometer equipped with Aspect 2000 computer using a Varian flat electrolytic cell with a platinum net working electrode. The corresponding EPR spectra were recorded during amperostatic polarisation and simulated using a standard Bruker program. The potential between the working and the reference electrodes was measured simultaneously. In experiments described below, spin traps were used in 0.01 mol dm^{-3} concentration.

Oxidation-initiated decomposition of probes 1, 3, 4, initiated by oxidizing agents like p-nitroperoxybenzoic acid (p-NPBA)[8] or Bu^{t}OO· radicals, prepared by decomposition of Bu^{t}OOH with PbO_2 as described in ref. 9 was carried out in benzene solutions. In standard experiments oxidising agents were added to a 0.01 mol dm^{-3} probe in benzene solution and EPR spectra recorded. The g-values were determined by means of a marker which is built into the spectrometer with an estimated accuracy ± 0.0001.
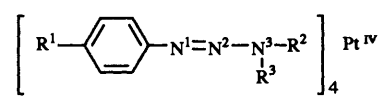
Results and discussion

Triazenes and their Pt complexes in prospective applications are exposed to various redox agents. The mechanism of their action is assumed to proceed via radical intermediates. Therefore, we characterised their redox properties by means of cyclic voltammetry, evaluated the corresponding oxidation and reduction peak potentials and degree of reversibility. The reduction or oxidation was considered here to be irreversible in the sense that on the reversal of the sweep no corresponding peak was found due to the fast consecutive reaction. The radical

Table 1 Structural formulae of the investigated triazenes (1, 2) and their Pt-complexes (3, 4) and the cyclovoltammetric data obtained in 0.001 mol dm^{-3} substrate, 0.1 mol dm^{-3} TBAP acetonitrile solutions (scan rate 500 mV s^{-1}; vs. SCE)^a

$$R^1\!\!-\!\!\left\langle\bigcirc\right\rangle\!\!-\!\!N^1{=}N^2{-}N^3{-}R^2$$
$$\underset{R^3}{|}$$

Substrates 1, 2

$$\left[R^1\!\!-\!\!\left\langle\bigcirc\right\rangle\!\!-\!\!N^1{=}N^2{-}N^3{-}R^2\right]_4 Pt^{IV}$$
$$\underset{R^3}{|}$$

Substrates 3, 4

Substrate	R^1	R^2	R^3	E_{pc}^{1}	$E_{pa}^{1'}$	$E_{pa}^{2'}$	E_{pa}^{1}	E_{pa}^{2}	E_{pc}'
1a	H	C$_6$H$_{13}$	H	−2.1	−0.1	−0.12	1.46	1.8	
1b	C$_4$H$_9$	C$_6$H$_{13}$	H	−1.9	0.0	−0.10	1.07	1.8	
1c	CN	C$_4$H$_9$	H	−1.95	−0.6	0.21	1.68	2.4	
1d	CN	C$_6$H$_{13}$	H	−1.95	−0.35	0.23	1.66	2.3	
1e	CN	C$_8$H$_{17}$	H	−1.95	−0.4	0.23	1.65		0.35
1f	CN	C$_{12}$H$_{25}$	H	−1.95	−0.5	0.22	1.70		0.35
1g	NO$_2$	C$_6$H$_{13}$	H	−1.48	−0.4	0.20	1.47	1.9	−0.3
2a	H	CH$_3$	OH	−2.3	—	−0.18	1.4	2.0	−0.3
2b	C$_4$H$_9$	CH$_3$	OH	−2.7	—	−0.23	1.16	1.8	−0.25
2c	CH$_3$O	CH$_3$	OH	−2.7	—	−0.30	1.03	1.8	−0.4
2d	CN	CH$_3$	OH	−2.1	−0.4	0.19	1.53	2.0	−0.15
2e	C$_4$H$_9$	C$_6$H$_{11}$	OH	—	−0.5	−0.16	1.35	2.2	−0.5
3a	H	C$_6$H$_{13}$	b	−2.1	0.25		0.85	1.16	−0.2
3b	CN	C$_6$H$_{13}$	—	−1.37 / −1.6^c	−1.05	−0.87	1.2		1.0
3c	NO$_2$	C$_6$H$_{13}$	—	−1.2 / −1.5^c	−1.25		1.2	1.46	
4	C$_4$H$_9$	CH$_3$	O	−2.7			0.73^d	1.63	0.6 / 1.4

^{a} E_{pa}^{1} anodic peak potential of the first oxidation peak; E_{pa}^{2} anodic peak potential of the second oxidation peak; E_{pc}' cathodic peak potential of the peak of the reverse scan; E_{pc}^{1} cathodic peak potential of the first reduction peak; $E_{pa}^{1'}$ anodic peak potential of the first peak on reverse scan; $E_{pa}^{2'}$ anodic peak potential of the second peak on reverse scan. ^{b} After H$^+$ abstraction R^3 formally represented by negative charge. ^{c} Second reduction peak. ^{d} Reversible (all other processes presented in Table 1 were irreversible).

products formed in the electrochemically initiated reactions of triazenes and in oxidation with peroxy acid and peroxyl radicals were then characterised by means of EPR spectroscopy.

Cyclic voltammetry

The cathodic and anodic peak potentials along with the peakpotentials observed in reverse scans and the reversibility degree extracted from cyclic voltammograms are summarised in Table 1.

Cathodic reduction. Triazenes 1a–f were irreversibly reduced at a potential around −1.95 V vs. SCE as illustrated in Fig. 1(a) for compound 1d. Triazene 1a with R^1 = H is reduced at a more negative potential (−2.1 V) than triazenes 1c–f with R^1 = CN (−1.95 V) reflecting the acceptor properties of the cyano group. During the reverse scans no corresponding counter peaks were found. Two peaks shifted about 2 V from the primary cathodic peak to the more positive potential indicating the formation of at least two consecutive products in this case. Upon increasing the scan rate from 500 to 20 000 mV s^{-1} no significant change in the reversibility of the reduction peaks was observed, implying very rapid consecutive reactions. Probe 1g with the p-NO$_2$ substituted phenyl ring was reduced at the most positive reduction potential (−1.48 V) owing to the strong acceptor effect of the NO$_2$ group. Hydroxylamine derivatives 2a–e differ from those with the –NH– group (1a–g). The reduction of 2a–e proceeds at more negative potentials than that of 1a–g and interferes with the decomposition of the electrolyte. The reduction potentials E_{pc}^{1} of 2a–e are in the range −2.1 to −2.7 V (Table 1), and depend on the R^1 and R^2 substituents. Probes 3a–c, 4 represent platinum(IV) centred complexes with triazenido ligands originating from triazenes 1a, 1d, 1g and 2b, respectively. Complexes 3a and 4 have the same reduction potentials as the corresponding triazenes 1a (−2.1 V) and 2b (−2.7 V). This implies that the observed reduction peaks reflect an irreversible reduction of the

ligand possibly associated with changes in the stereochemistry of Pt complexes. On the other hand, complex 3b with p-CN substituted and complex 3c with a p-nitro substituted phenyl ring in the triazenido ligand show two reduction peaks, the first being at the potential −1.37 V (3b) and −1.2 (3c) and the second at −1.6 V (3b) and −1.5 V (3c). The second peak for compounds 3c has a counter peak shifted to the more positive potential about 300 mV [Fig. 2(a)]. The formation of a stable anion radical in the region of the second reduction peak from modified leaving ligand was observed using the EPR technique described below. Consequently, the first reduction peak probably represents the platinum reduction associated with the loss of ligands[10] whereas the second step corresponds to the reduction of the ligand released.

Anodic oxidation. All triazenes 1a–g, 2a–e generally show two oxidation peaks as illustrated in Fig. 1(b) for triazene 1d. As found in the cathodic reduction, in the anodic oxidation an influence of R^1 and R^2 on the first oxidation peak potentials in agreement with their donor–acceptor properties was observed. Thus, E_{pa}^{1} = 1.46 V for unsubstituted triazene 1a increased to around 1.65 V by CN-substitution (1c–f) and decreased to 1.07 V if R^1 = C$_4$H$_9$ (1b). The oxidation potentials of hydroxy-substituted triazenes 2a–e are 1.0–1.5 V. If anodic oxidation was carried out in the presence of Bu^{t}NO spin trap, EPR spectra of radical adducts were observed in the region of the first oxidation peak as described below. In Pt-complexes 3a, 3b and 4, the potential of the first oxidation peak was decreased by about 0.5 V, when compared with the corresponding free ligands 1a, 1d and 2b. The second oxidation peaks are also considerably lower than in non-complexed triazenes and their intensities decrease with increasing scan rates. Consequently, they may be assigned to consecutive products. Complex 4 showed reversible behaviour for both peaks, whereas both peaks of 3a–c behaved irreversibly as illustrated with the cyclic voltammogram of 3c in Fig. 2(b).
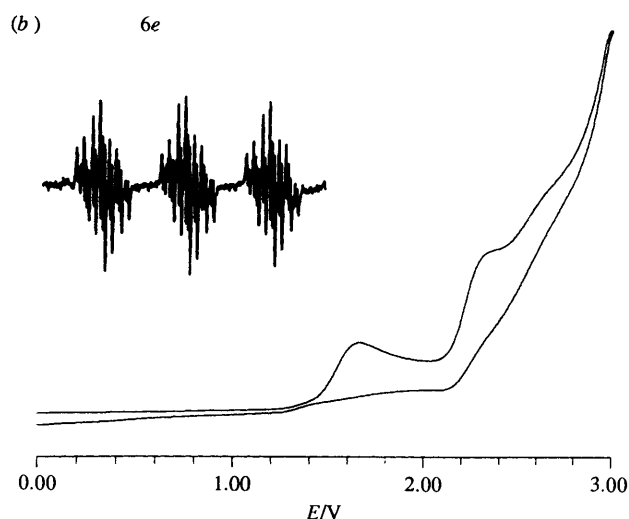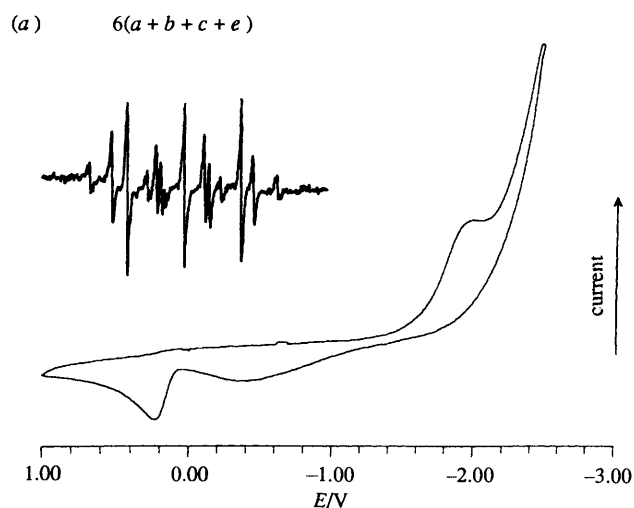
(a)   6(a + b + c + e)

(a)   exper.   5   simulat.

(b)   6e

(b)   exper.   6f   simulat.

Fig. 1 Cyclic voltammograms observed in the cathodic reduction (a) and anodic oxidation (b) of 0.001 mol dm⁻³ triazene **1d** and 0.1 mol dm⁻³ TBAP acetonitrile solution (scan rate 500 mV s⁻¹, potentials are in volts vs. SCE), along with EPR spectra obtained using Bu^{t}NO spin trap [insets of Figs. 1(a,b)]

Fig. 2 Cyclic voltammograms found in the cathodic reduction (a) and anodic oxidation (b) of 0.001 mol dm⁻³ Pt-complex **3c** and 0.1 mol dm⁻³ TBAP acetonitrile solution (scan rate 500 mV s⁻¹, potentials in volts vs. SCE), along with experimental (low-field half) and simulated (high-field half) EPR spectra obtained without Bu^{t}NO (inset of a) and using Bu^{t}NO spin trap (inset of b)

Simultaneous electrochemical–EPR experiments

Cathodic reduction. Generally, in the primary and secondary reduction steps, probes 1–4 showed no counter peaks and no radicals were found in EPR investigations. Only sample **3c** exhibits a counter peak at the second reduction step, slightly shifted to more positive potential (300 mV) and a stable anion radical **5** was observed, the spectrum of which is shown in Fig. 2(a). From its simulation a para-substituted nitrobenzene anion radical is evident with: $2 \times a_H{}^m = 0.115$ mT, $2 \times a_H{}^o = 0.34$ mT, $a_N(NO_2) = 1.221$ mT, $a_N = 0.11$ mT, $a_N = 0.098$ mT and $a_N = 0.007$ mT. The lowest splitting constant (0.007 mT) was not directly evident from the hyperfine structure, but it was necessary to take it into account in the simulation to fit the experimental line shape. This implies that after the first irreversible reduction step, the platinum complex **3c** undergoes a rapid conversion (possibly Pt^{IV} reduction and release of ligand [10]). The ligand is subsequently reduced with the formation of anion radical p-O₂N–C₆H₄–N=N–NR²–Z⁻˙ with unpaired spin density centred on the nitro group, where Z is abstracted from the surroundings. Another alternative cannot be excluded: the elimination of two nitrogens and formation of the corresponding cage product.

The electrochemical irreversibility of the first reduction step of probes 1–4 and the absence of radical products in EPR experiments indicate a rapid consecutive conversion of the radical anions formed. Therefore, experiments were carried out
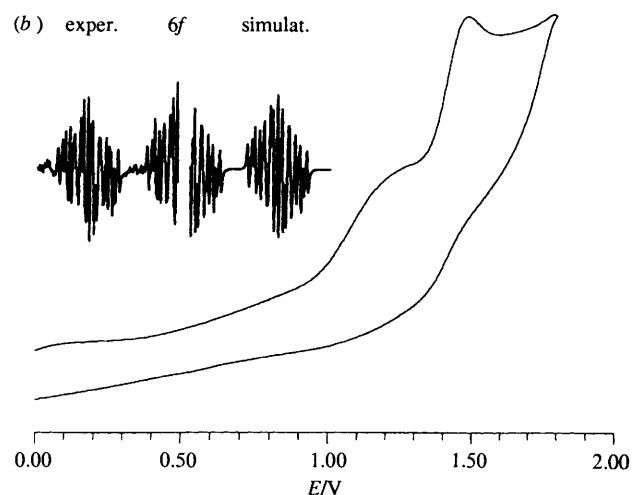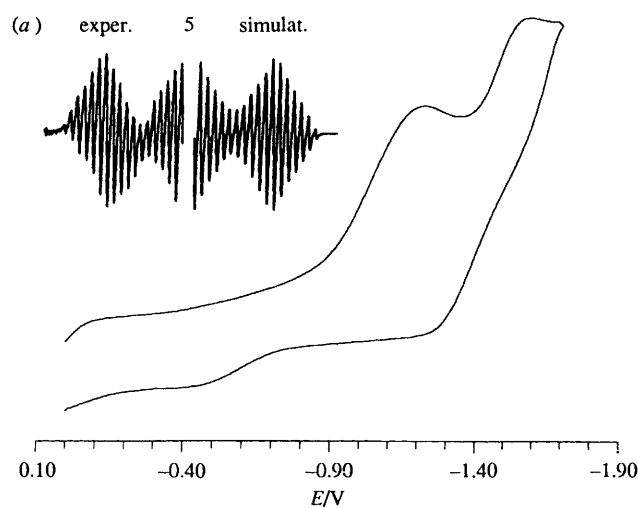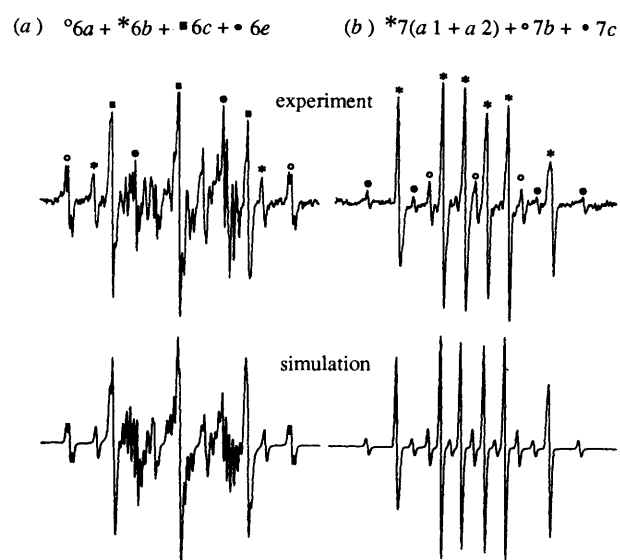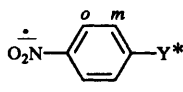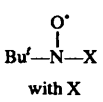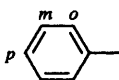
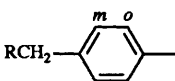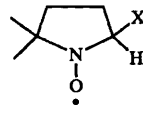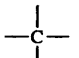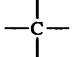(a)   °6a + *6b + ■6c + • 6e   (b)   *7(a 1 + a 2) + °7b + • 7c
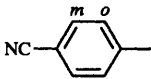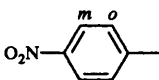
Fig. 3 Experimental and simulated EPR spectra of spin adducts obtained in the cathodic reduction of triazene **1e** using Bu^{t}NO (a) and triazene **1c** with DMPO (b)

Table 2 Splitting constants and their assignment to the radicals **5–7** observed in the cathodic reduction ($+e^-$), anodic oxidation ($-e^-$) of substrates **1–4**

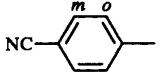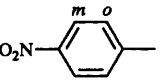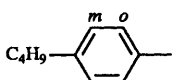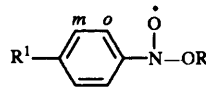|	Structure	Splitting constant mT	Generation/Solvent/From
5	•O₂N—[benzene ring, o m]—Y*	$a_{N(NO_2)}$ 1.221, $2a_H^o$ 0.34, $2a_H^m$ 0.115	$+e^-$ red./ACN/**3c**
	Y* probably N=N—N—R²Z	$3a_N(Y)$ 0.11, 0.098, 0.007	
6	O• / Bu^t—N—X with X	In the presence of 'BuNO	
6a	—CH₂CH₂R	$a_{N(NO)}$ 1.61, $2a_H$ 1.022, $2a_H$ 0.06	$+e^-$ red./ACN/**1a–g**
6b	H	$a_{N(NO)}$ 1.375, a_H 1.246	$+e^-$ red./ACN/**1–4**
6c	Bu^t	$a_{N(NO)}$ 1.53	$+e^-$ red./ACN/**1–4**
6d	p[benzene ring, m o]	$a_{N(NO)}$ 1.48, $3a_H^{o,p}$ 0.19, $2a_H^m$ 0.094	$-e^-$ ox./ACN/**1a, 2a, 3a** $+e^-$ red./ACN/**1a**
6e	NC—[benzene ring, m o]	$a_{N(NO)}$ 1.138, $2a_H^o$ 0.173 $2a_H^m$ 0.093, $a_{N(CN)}$ 0.0317	$-e^-$ ox./ACN/**1c–f, 2d, 3b** $+e^-$ red./ACN/**1c–f**
6f	O₂N—[benzene ring, m o]	$a_{N(NO)}$ 1.08, $2a_H^o$ 0.223, $2a_H^m$ 0.092, $a_{N(NO_2)}$ 0.057	$-e^-$ ox./ACN/**1g, 3c** $+e^-$ red./ACN/**1g**
6g	RCH₂—[benzene ring, m o]	$a_{N(NO)}$ 1.32, $2a_H^o$ 0.212, $2a_H^m$ 0.095, $a_{H(CH_2)}^p$ 0.127	$-e^-$ ox./ACN/**1b, 2b, e** $+e^-$ red./ACN/**1b**
7	[pyrroline ring with X, N–O•, H] with X	In the presence of DMPO	
7a 1	—C—	$a_{N(NO)}$ 1.54, a_H 2.255	$+e^-$ red./ACN/**1–2**
7a 2	—C—	$a_{N(NO)}$ 1.485, a_H 2.21	$+e^-$ red./ACN/**1**
7b	?	$a_{N(NO)}$ 1.567	$+e^-$ red./ACN/**1**
7c	?	$a_{N(NO)}$ 2.9, a_H 1.582	$+e^-$ red./ACN/**1**
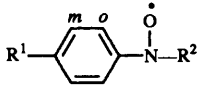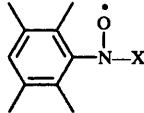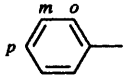
in the presence of 2-methyl-2-nitrosopropane as a spin trap (Bu^tNO). The inset in Fig. 1(*a*) presents the superimposed EPR spectra found in the reduction of **1d**. Fig. 3(*a*) (representative for triazenes **1a–g**) shows experimental and simulated EPR spectra of spin adducts, X–NO•–Bu^t, observed in the region of the first cathodic reduction peak of **1e**. The spectra obtained usually represent an accumulation of 10–20 scans due to the low yield and stability of spin adducts formed. The simulated splitting constants are summarised in Table 2. Four radical species were identified in Fig. 3(*a*) (**6a,b,c,e**). The spin trap itself contributed two radicals Bu^t–NO•–Bu^t (**6c**—admixture of trap) and Bu^t–NO•–H (**6b**—formed in H-abstraction from surroundings). Two further adducts **6a** with R–CH₂CH₂• and **6e** with *p*-CN–C₆H₄• are evidently direct fragmentation products in the cathodically initiated decomposition of triazene.

With TBAP as the electrolyte, the expected alkyl group (R–CH₂CH₂–) could also be butyl (C₂H₅CH₂CH₂–) origin-ating from tetrabutylammonium cation. This alternative was eliminated using LiClO₄ as a support salt where formation of the R–CH₂–CH₂–NO•–Bu^t adduct was also confirmed.

Fig. 3(*b*) shows experimental and simulated EPR spectra observed in the cathodic reduction of **1c** in the presence of the DMPO spin trap. Such spectra are characteristic of triazenes **1a–g** presented in Table 2. Two carbon-centred radicals added to DMPO (**7a1**) with a_H = 2.255 mT and a_N = 1.54 mT and (**7a2**) with a_H = 2.21 mT and a_N = 1.485 mT, are obvious. This is in agreement with the formation of two radicals *p*-R¹–C₆H₄• and R–CH₂–CH₂• described in the experiments with Bu^tNO. Two further adducts X–DMPO• (**7b** with a_N = 1.567 mT) and Y-DMPO• (**7c** with a_H = 1.582 mT and a_N = 2.9 mT) are evident from Fig. 3(*b*). X–DMPO• is frequently assumed to be a product of the multiple radical attack on DMPO, abstracting hydrogen in position 2 from the pyrroline skeleton. The formation of the further Y–DMPO• adduct, with an unusually

Table 3 Splitting constants and their assignment to the radicals 8–10 observed in the oxidation of substrates 1–4 with p-NPBA, $Bu^tOOH + PbO_2$

Structure		Splitting constant mT	Generation/Solvent/From
8	R^1—⟨C_6H_4⟩—N(—O·)—R^2 $R^2 = CH_2$—R with R^1		
8a	H–	$a_{N(NO)}$ 1.060, $3a_H^{o,p}$ 0.288, $2a_H^m$ 0.090, $2a_{H(CH_2)}$ 0.724	p-NPBA/benzene/1a
8b	NC–	$a_{N(NO)}$ 0.955, $2a_H^o$ 0.265, $2a_H^m$ 0.097, $2a_{H(CH_2)}$ 0.705, $a_{N(CN)}$ 0.040	p-NPBA/benzene/1c–f
8c	C_4H_9–	$a_{N(NO)}$ 1.065, $2a_H^o$ 0.290, $2a_H^m$ 0.098, $2a_H^p$ 0.222, $2a_{(CH_2)}$ 0.720	p-NPBA/benzene/1b
9	(dimethyl ring) N(—O·)—X with X	in the presence of ND	
9a	—CH_2R	$a_{N(NO)}$ 1.36, $2a_H$ 1.07	p-NPBA/benzene/1a–f
9b	p (phenyl)	$a_{N(NO)}$ 1.01, $3a_H^{o,p}$ 0.275, $2a_H^m$ 0.085	p-NPBA/benzene/1a, 3a
9c	NC–	$a_{N(NO)}$ 0.990, $2a_H^o$ 0.275, $2a_H^m$ 0.090	p-NPBA/benzene/1c–f, 3b
9d	O_2N–	$a_{N(NO)}$ 0.990, $2a_H^o$ 0.275, $2a_H^m$ 0.090	p-NPBA/benzene/3c
9e	C_4H_9–	$a_{N(NO)}$ 1.028, $2a_H^o$ 0.285, $2a_H^m$ 0.090, $a_{H(CH_2)}^p$ 0.215	p-NPBA/benzene/1b
10	R^1—⟨C_6H_4⟩—N(—O·)—OR with R^1		
10a	H–	$a_{N(NO)}$ 1.430, $3a_H^{o,p}$ 0.295, $2a_H^m$ 0.090	$Bu^tOOH + PbO_2$/benzene/1a
10b	NC–	$a_{N(NO)}$ 1.280, $2a_H^o$ 0.298, $2a_H^m$ 0.103, $a_{N(CN)}$ 0.043	$Bu^tOOH + PbO_2$/benzene/1c–f
10c	C_4H_9–	$a_{N(NO)}$ 1.490, $2a_H^o$ 0.295, $2a_H^m$ 0.097, $2a_H^p$ 0.220	$Bu^tOOH + PbO_2$/benzene/1b

high nitrogen splitting constant is not explained at present. In the cathodic reduction of platinum complexes 3a and 3b in the presence of spin traps no adducts originating from triazene fragments were observed.

Anodic oxidation. On the direct oxidation of probes 1a–g, 2a–e in the cavity of the EPR spectrometer no radical products were found. Therefore, further experiments were carried out in the presence of the Bu^{t}NO trap. High yields of p-R^1–C$_6$H$_4$–NO$^•$–Bu^t adducts, 6d–g, (Table 2) formed at the potential of the first oxidation peak were obtained from all of the above mentioned triazenes. Fig. 4(a) illustrates this with the EPR spectrum of the p-CN–C$_6$H$_4$–NO$^•$–Bu^t adduct (6e) observed during oxidation of 1d. The corresponding splitting constants from other adducts are summarised in Table 2. Upon oxidation of Pt complexes the radical adducts were also found, but in a considerably lower yield than with the corresponding triazenes. This illustrates the spectrum of radical adduct 6f p-NO$_2$–C$_6$H$_4$–NO$^•$–Bu^t shown in the inset of Fig. 2(b) generated in the oxidation of 3c, its parameters are given in Table 2.

The electrochemical and EPR investigations demonstrate the different behaviours of free and platinum co-ordinated triazenes. Free triazenes in the first reduction or oxidation step form unstable radicals which rapidly decompose under N$_2$ elimination. To explain the formation of the observed radicals two tautomeric forms of the investigated triazenes have to be assumed as described in Scheme 1. The radicals given there can recombine to secondary amines, which can then be oxidised as indicated by the cyclic voltammetry. The absence of the adduct R^2–NO$^•$–Bu^t during the anodic oxidation implies that the decomposition is predominantly initiated on N^3. On the other hand the triazenes in platinum complexes do not form radical adducts during the electrochemical reduction and only low yields of adducts were found in the anodic oxidation. In summary, there are two different forms of triazene investigated. The free triazene which has a NH group and then triazene as a ligand without hydrogen due to the formation of the corresponding anion. The complexation of triazenes with platinum results in their increased stability in redox reactions and is probably the reason for the differing behaviour in the reduction of free triazene and its complexed form.
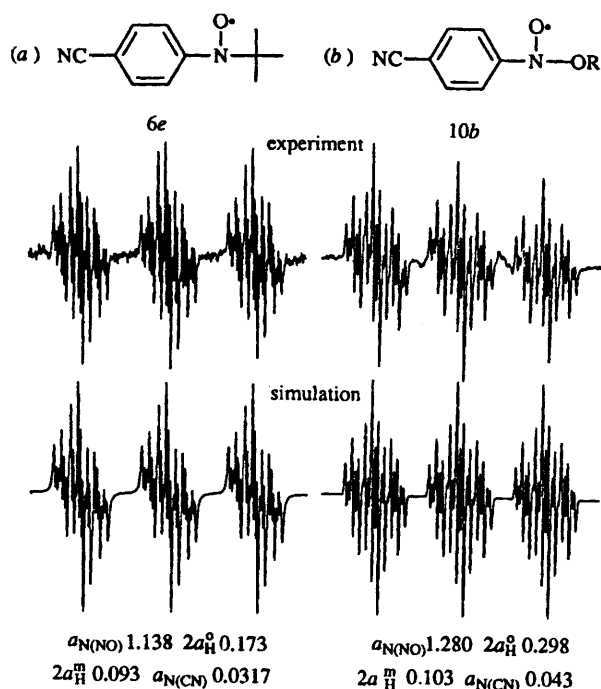
(a) NC—⟨benzene⟩—N(O•)—$\dagger$ (b) NC—⟨benzene⟩—N(O•)—OR

6e   *10b*

experiment

simulation

$a_{N(NO)}$ 1.138 $2a_H^o$ 0.173 $a_{N(NO)}$ 1.280 $2a_H^o$ 0.298

$2a_H^m$ 0.093 $a_{N(CN)}$ 0.0317 $2a\,_H^m$ 0.103 $a_{N(CN)}$ 0.043

Fig. 4 Experimental and simulated EPR spectra of radicals obtained in the anodic oxidation of triazene **1d** (*a*) in the presence of Bu^{t}NO spin trap and in the oxidation of triazene **1c** with Bu^{t}OO• (*b*)

8b   *9a*   *9b*

(a) NC—⟨benzene⟩—N(O•)—(CH₂)₃—CH₃ (b) Dur—N(O•)—(CH₂)₃—R   +   Dur—N(O•)—C₆H₅

experiment

simulation

$a_{N(NO)}$ 0.9552 a_H^o 0.265 $a\,_H^m$ 0.097 $a_{N(NO)}$ 1.36 $2a_H^o$ 1.07(*9a*)

$2a_{H(CH_2)}$ 0.705 $a_{N(CN)}$ 0.040 $a_{N(NO)}$ 1.01 $3a_H^{o,p}$ 0.275 $2a_H^m$ 0.085 (*9b*)
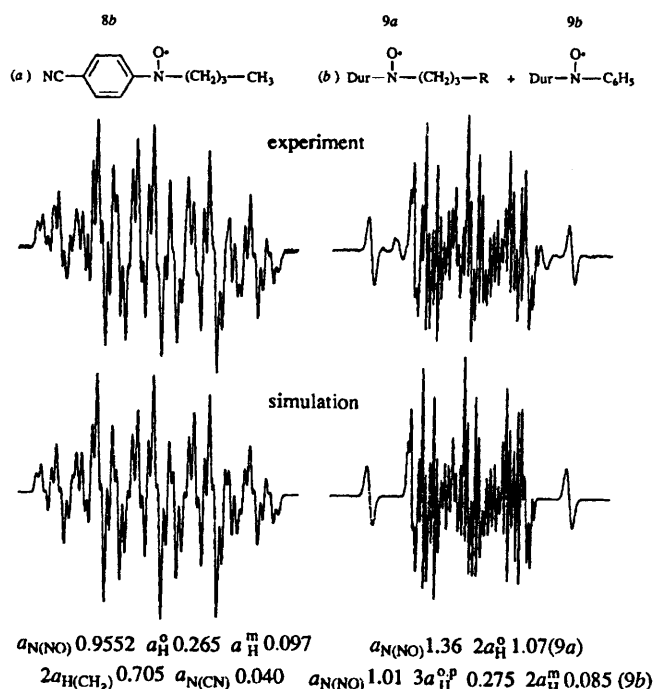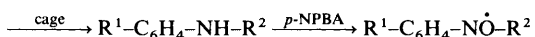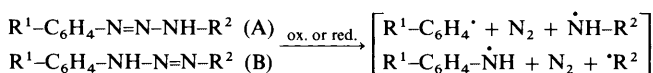
Fig. 5 Experimental and simulated EPR spectra of radicals obtained in the oxidation of triazene **1c** with *p*-NPBA (*a*) and in the oxidation of triazene **1a** with *p*-NPBA in the presence of ND spin trap (*b*).

Radical intermediates in chemical oxidation (EPR spectroscopy)

Oxidation with *p*-NPBA. In the oxidation of triazenes **1a–f**, EPR spectra were observed, which can be attributed to the nitroxyl radicals **8** with the common formula *p*-R^1-C$_6$H$_4$-NO•-R^2. Fig. 5(*a*) presents experimental and simulated spectra of **8b** found in the oxidation of triazene **1c**. The parameters of other nitroxyls **8** observed are summarised in Table 3.

To obtain more information on the decomposition mechanism, oxidations with *p*-NPBA were also carried out in the presence of ND spin trap. The experimental and simulated spectra obtained from **1a** are shown in Fig. 5(*b*) where two radical adducts •CH$_2$R (**9a**) and •Ph (**9b**) are evident. The formation of •R^2, *p*-R^1-C$_6$H$_4$• can be explained by standard fragmentation of azo compounds, assuming two tautomeric forms (A,B) of triazenes and *p*-R^1-C$_6$H$_4$-NO•-R^2 by the consecutive reactions according to Scheme 1.

R^1-C$_6$H$_4$-N=N-NH-R^2 (A) $\xrightarrow{\text{ox. or red.}}$ [R^1-C$_6$H$_4$• + N$_2$ + •NH-R^2

R^1-C$_6$H$_4$-NH-N=N-R^2 (B)   R^1-C$_6$H$_4$-ṄH + N$_2$ + •R^2]

$\xrightarrow{\text{cage}}$ R^1-C$_6$H$_4$-NH-R^2 $\xrightarrow{p\text{-NPBA}}$ R^1-C$_6$H$_4$-ṄO-R^2

Scheme 1

Evidence for tautomeric forms A, B was found in ref. 5. Oxidation-initiated decomposition probably proceeds *via* *p*-R^1-C$_6$H$_4$N$_2$• or •N$_2$R intermediates, finally forming *p*-R^1-C$_6$H$_4$• and •R^2 radicals. These, in the presence of ND, are trapped during the formation of the observed adducts **9** (Table 3). From the intermediates [*p*-R^1-C$_6$H$_4$•, •R$_2$, *p*-R^1-C$_6$H$_4$-NH• and •NHR^2] the formation of cage products, secondary amines, *p*-R^1-C$_6$H$_4$-NH-R^2, is expected. Secondary amines are known to form nitroxyl radicals in oxidation with peroxy acids,[8] similar to what was observed in our experiments.

In a direct oxidation of triazenido platinum complexes **3a–c** with *p*-NPBA, no radicals were observed. Therefore, further experiments were also carried out in the presence of ND. As

mentioned above triazenes **1a–f** form two adducts *p*-R^1-C$_6$H$_4$ND• and R^{2}ND• whereas their P complexes form only one adduct *p*-R^1-C$_6$H$_4$ND•. The absence of the second adduct R^{2}ND• can be explained assuming that in the corresponding Pt-complexes (*p*-R^1-C$_6$H$_4$-N=N-N$^-$-R^2)$_4$Pt^{IV}, the oxidation is predominantly initiated on the negatively charged N^3, probably forming *p*-R^1-C$_6$H$_4$N$_2$• intermediates and then, under N$_2$ elimination, *p*-R^1-C$_6$H$_4$• radicals.

Oxidation with Bu^{t}OO• radicals. In the oxidation of triazene **1c** a nitroxyl radical **10b** was found with the EPR spectrum shown in Fig. 4(b), which is also representative of triazenes **1a–f**. From its simulation, the contribution of *p*-CN-C$_6$H$_4$-ring and -NO•- group to the hyperfine structure is evident. The *g*-value ($g = 2.0048$) and the absence of a further contribution to the hyperfine structure, implies that the second fragment is the RO- group (Bu^{t}O- or Bu^{t}OO-) and consequently the structure of the observed radical is *p*-R^1-C$_6$H$_4$-NO•-OR (**10b**). Its formation may be derived from Scheme 1 assuming recombination between RO• and *p*-R^1-C$_6$H$_4$-NH• radicals forming *p*-R^1-C$_6$H$_4$-NH-OR amines, which undergo a further oxidation to the corresponding nitroxyl radicals **10a–c** (Table 3). When the system PbO$_2$-Bu^{t}OOH was applied to the oxidation of Pt-complexes **3a–c**, only a singlet EPR spectrum ($g = 2.0147$) was observed characteristic of complexed Bu^{t}OO• radicals.[11] These facts indicate that peroxyl radicals are inactive towards the triazene ligands in platinum complexes. Similarly, as described in electrochemical redox reactions, the platinum co-ordinated triazene complexes resist decomposition initiated with peroxy compounds.

References

1 F. A. Benson, *The High Nitrogen Compounds*, Wiley, New York, 1984.

2 M. Bolle, K. Luther and J. Troe, *Appl. Surf. Sci.*, 1990, **46**, 279.

3 B. J. Foster, D. R. Nevell, J. Carmichael, A. L. Harris, L. A. Gumbrell, D. E. V. Wilman and A. H. Calvert, *Br. J. Cancer*, 1988, **58**, 276.

4 J. Dauth, B. Deubzer and U. Peetz, *Eur. Pat.* 602638 A1/1993.

5 R. H. Smith, Jr., B. D. Wladkowski, J. A. Herling, T. D. Pfaltzgraff,

B. Pruski, J. Klose and Ch. J. Michejda, *J. Org. Chem.*, 1992, **57**, 654.

6 (*a*) J. Huguet, M. Libert and C. Caullet, *Bull. Soc. Chim. Fr.*, 1972, **12**, 4860; (*b*) L. Dunsch, B. Gollas, A. Neudeck, A. Petr, B. Speiser and H. Stahl, *Chem. Ber.*, 1994, **127**, 2423.

7 J. Dauth, B. Deubzer and J. Weis, *J. Organomet. Chem.*, 1993, **459**, 359 and refs. cited therein.

8 T. Toda, E. Mori and K. Murayama, *Bull. Chem. Soc. Jpn.*, 1972, **45**, 1904.

9 L. Omelka, M. Reinhardt, R. Kluge and M. Schulz, *Collect. Czech. Chem. Commun.*, 1988, **53**, 243.

10 A. M. Bond, R. Colton, D. A. Fiedler, J. E. Kevekordes, V. Todesco and T. F. Mann, *Inorg. Chem.*, 1994, **33**, 5761.

11 A. Tkáč, K. Veselý and L. Omelka, *J. Phys. Chem.*, 1971, **75**, 2575.